



Human-in-the-loop control of guided airdrop systems

Martin R. Cacan^{a,*}, Mark Costello^a, Michael Ward^b, Edward Scheuermann^b,
Michael Shurtliff^c

^a Center for Advanced Machine Mobility, Georgia Institute of Technology, Atlanta, GA, 30322, USA

^b Earthly Dynamics Corporation, Atlanta, GA 30309, USA

^c Airdrop Technology Team, Natick Soldier Research, Development & Engineering Center, Natick, MA 01760, USA

ARTICLE INFO

Article history:

Received 8 March 2016

Received in revised form 20 January 2018

Accepted 6 August 2018

Available online 4 October 2018

Keywords:

Precision airdrop

Human operated

User interface

Autonomous system

ABSTRACT

Advances in guided airdrop technology including guidance, navigation, and control algorithms, novel control mechanisms and wind sensing algorithms have led to significant improvements over unguided airdrop systems. Guided systems are autonomously controlled with an embedded microprocessor using position and velocity feedback. While capable of highly accurate landing, these systems struggle to overcome deviations from expected flight dynamics due to canopy damage or cargo imbalance, complex terrain at the drop zone, and loss of sensor feedback. Human operators are intelligent, highly adaptive, and can innately judge the flight vehicle and environment to steer the vehicle to the desired impact point provided sufficient information. This work experimentally explores operators' abilities to accurately land an airdrop system using different sensing modalities. Human operator landing results are compared with a state of the art fully autonomous airdrop system. Across the methods analyzed, human operators attained up to a 40% increase in landing accuracy over the fully autonomous control algorithm.

© 2018 Elsevier Masson SAS. All rights reserved.

1. Introduction

Airdrop systems are generally categorized into guided or unguided systems. Unguided systems are typically released from low altitudes and descend to the ground without feedback or control. Landing accuracy of these systems is dependent on the drop altitude, the quality of atmospheric wind estimates, and the computed air release point [1,2]. Guided airdrop systems use either steerable round chutes [3,4] or ram air parafoils combined with sensor suites to provide controllability and observability, respectively. Early autonomous systems used directional antennas as a form of beacon guidance [5–8]. After the deployment of the original 24 satellites forming the backbone of the Global Positioning System (GPS), more advanced algorithms capitalized on the rich data available for feedback [9–15]. GPS feedback allows the autonomous system to estimate and reject the atmospheric winds making them more accurate than unguided systems and protecting the carrier aircraft by enabling high altitude release points. The primary disadvantage to these systems is the greater cost due to the need for sensors, actuators, and computing capabilities.

Both unguided and guided airdrop methods require no human intervention once released from the carrier aircraft. While this is a benefit in many active battlefield scenarios, any unaccounted disturbances or changes in expected system performance can drastically reduce system landing accuracy. For guided systems, such changes include deviations in the flight dynamics from the model (not uncommon for flexible systems), loss or denial of GPS feedback, low altitude wind shears, or requirements for obstacle avoidance due to complex terrain at the drop zone (DZ). While some of these problems are just recently being addressed in autonomy (see [16] for drop zone terrain considerations and [17] for overcoming wind shears), a middle ground between guided and unguided systems exists which incorporates a human operator to steer the airdrop system to the desired impact point (IP). The benefits of this type of approach stem directly from a human operator's innate ability to adapt to changing situations, employ forward path prediction, and be unconstrained from often rigid, pre-defined control logic. In addition, this human-in-the-loop approach mimics how current military drone operations are conducted in the field today.

Significant work exists in the literature on human-in-the-loop control schemes between humans and robotic systems. Research primarily focuses on ground based platforms with examples ranging from inner loop autonomous stability constraints for legged robots [18,19] to haptic feedback systems [20–22]. For aerial ve-

* Corresponding author.

E-mail address: martincacan@gatech.edu (M.R. Cacan).

hicles, most initial flight testing of autonomous systems have a human pilot ready to take over control if an error occurs. An available human represents an intelligent, highly adaptive control system to ensure the system can still be recovered. An initial study into the benefits of human control of guided airdrop systems was tested by Mayer et al. [23,24] in the 1980's. Since the implementation of GPS, human-in-the-loop control strategies in aerospace have focused on fixed-wing vehicles [25–29] or the control of multiple platforms by a single operator [30,31] due to a document issued by the Office of the Secretary of Defense outlining future goals of unmanned aerial vehicles [32]. The visual feedback methods studied here combine elements common to remote piloting of fixed wing UAVs which are prevalent in both military and hobbyist communities. Fixed wing displays are commonly designed to mimic a cockpit experience using video feedback with overlaid pitch, roll, heading, altitude and other indicators including projected path estimates [25–29]. However, there are significant differences between the dynamics and control of fixed wing aircraft and guided parafoil systems that limit the transition of previously studied displays to this work. First, these vehicles lack thrust generation which limits the forward airspeed while having relatively constant descent rates (common ram air parafoils have a glide slope of 3 to 1). Low vehicle airspeed makes the flight trajectory highly dependent on the atmospheric wind conditions. Minimal control authority of the descent rate causes the terminal phase of landing to happen quickly and provides operators only one opportunity to line up for landing. Additionally, these systems have relatively poor feedback (typically just GPS) which prevents many of the common indicators like bank angle from being utilized.

This work seeks to explore the impact of integrating a human pilot into typically autonomous operations. The capabilities of several human-in-the-loop control strategies for guided parafoil systems are compared with a state of the art autonomous algorithm. Operators' abilities are measured through statistical analysis of experimental flight test results conducted on a small-scale airdrop system. To study the capabilities of a human operator and specifically what type of system interface is most useful, a series of sensing and control modalities are explored. First, an on-site method was tested where the operator is located near the IP and looks upward to visually track the motion of the airdrop system during gliding descent. This method mimics how conventional remote control (CRC) aerial vehicles are steered in the hobby community and provides a baseline for other concepts. The remaining methods use wireless communication to transmit vehicle data and/or a video stream to a ground station computer. These three methods are termed first person view (FPV) video stream, live map (LM) interface, and virtual cockpit display (VCD). The FPV method uses a camera rigidly mounted to the nose of the payload to provide a first person view from the aerial vehicle. The goal is to replicate a skydiver's perspective and allow the ground based human operator to make decisions as if they were physically flying the aerial vehicle. The LM interface uses navigation estimates to generate a bird's eye view map of the DZ with the airdrop system, heading direction, and wind estimates displayed. This method provides the user with a clear understanding of the orientation and position of the vehicle as if flown from above instead of below as in the CRC method. The last method combines the FPV and LM methods to create a virtual cockpit display. This method focuses on fusing the independent data streams together in a comprehensive display to allow operators to make the most informed control decisions. Between these four methods which consider both on-site and remote pilot methods, this work addresses the primary means and ways in which a human operator can remotely control a conventionally autonomous airdrop system.



Fig. 1. Small-scale airdrop system used in experimental testing.

2. Experimental setup

To conduct experimental results on the proposed methods, a small-scale remote control airdrop system is employed. The payload is equipped with an autopilot, servo motors, electric brushless motor, speed controller, battery, GoPro camera and wireless video transmitter. Fig. 1 shows a close up of the payload with associated hardware along with a picture during flight. The autopilot runs a PIC32MX family microcontroller and contains a sensor suite including a barometric altimeter and GPS receiver. Flight data is stored in EEPROM onboard memory and transmitted down to a base station computer via a wireless link for use in the feedback displays. Lateral control through trailing edge deflection of the canopy is provided by two high torque servo motors. Power is provided to payload electronics from a 6000 mAh lithium polymer battery, sufficient to power the system over two complete flights. The rear mounted motor and propeller are included to facilitate experimental testing using a 'simulated drop' method. For this, the system is hand launched from ground level, flown under power to gain altitude until a desired 'release' altitude is reached at which time the motor is turned off and the human operator or comparator autonomous algorithm is given control of the vehicle. Release altitude was chosen to be 400 m which allowed approximately 3 minutes of flight per drop. A high torque servo winch is installed to decrease the canopy incidence angle during powered flight to prevent stall. Lastly, the GoPro camera is mounted at the front of the payload, angled down to provide a view of the space in front and below the system. Recorded video is transmitted to the base station computer to provide a real time video feed from the airdrop system.

Control of the vehicle for powered climb and gliding descent is provided through a 2.4 GHz radio controller commonly used in hobby communities. The 7-channel controller gives the operator control over thrust, canopy incidence angle, low to high turn rate settings, symmetric and asymmetric brakes, data logging and a switch to engage the fully autonomous mode. The configuration of the controller is shown in Fig. 2. During descent, the pilot only uses the right stick to control asymmetric and symmetric brake deflection which affects the lateral and longitudinal dynamics, respectively. For all tests, human operators were given the following objectives:

1. Attempt to land as close to the target as possible;
2. Ensure payload survivability by maintaining level flight with the system flying directly into the wind just prior to impact; and
3. Avoid collision of the airdrop system with any obstacles near the DZ.

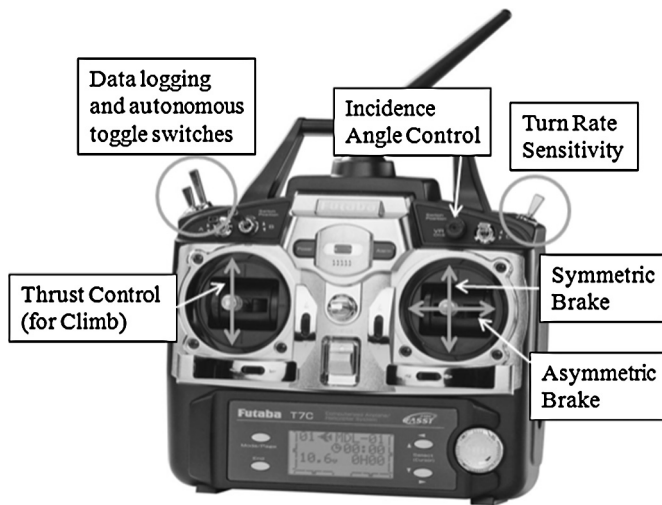


Fig. 2. Human operator interface for control of a guided airdrop system.

These objectives prioritize both landing accuracy and payload survivability. By landing directly into the wind during straight and level flight, the ground speed of the airdrop system is minimized which reduces the kinetic energy prior to impact. While highly aerobatic maneuvers close to the IP may reduce landing error, significant damage can occur to the payload. Note that while the human operator is able to actively attempt to satisfy objective 3 based upon feedback information received, the fully autonomous system is blind to any potential obstacle near the IP.

It is expected that several key elements will factor into the pilots ability to accomplish the mission objectives listed above. They are:

1. Form and fidelity of the feedback method;
2. Experience of the operator, both in remote control aircraft and the field of guided parafoil systems; and
3. Atmospheric weather condition.

This highlights the multivariable nature of the problem being addressed here. The first point is the primary focus of analysis in this paper. The experience of the operators will impact their decision making as less trained operators will be more prone to making poor decisions. Operators' skill level is ranked from novice to expert based on experience in radio control aerial systems or guided parafoil systems in general and amount of previous flight time using the small-scale experimental vehicle. While variation in skill amongst operators may skew landing accuracy statistics, the goal is to understand both quantitative and qualitative aspects of a successful human interface. Last, atmospheric conditions are a major concern for both human operators and autonomous algorithms alike and by concurrently testing both, the influence of atmospheric winds on relative performance can be minimized.

3. Feedback methods for human-in-the-loop control

With a focus on identifying key aspects of feedback to a ground based human operator, four methods are analyzed ranging from visually spotting the aerial system in the sky directly to multi-element digital displays. Each of the four feedback methods for human-in-the-loop control and the baseline fully autonomous algorithm are presented in detail in the following sections.

3.1. Fully autonomous

A modern, GPS based airdrop guidance, navigation, and control (GNC) algorithm is used as a comparator to human-in-the-loop

control methods presented in this work. A lateral steering controller based on the work in [33] is used and a brief summary of the algorithm is presented here as a reference.

The navigation algorithm filters GPS and barometric altimeter measurements using standard and extended Kalman filters to generate accurate estimates of the airdrop system position, velocity, heading, heading rate and horizontal components of the atmospheric winds. To accurately initialize the navigation algorithm, a short open loop initialization phase is used to generate an estimate of the navigation state vector to ensure accurate convergence of the observer [34]. The guidance algorithm uses the navigation estimates to generate desired paths which maintain general proximity to the target while at altitude and end at the IP when there is expected to be zero altitude. Path planning in the guidance algorithm is broken into 4 sections based on the current goals of the airdrop system. The system starts in an initialization period required by the navigation algorithm and then actively loiters in the airspace above the DZ. When the current altitude is equal to the altitude required to reach the IP (based on distance, heading, altitude, and wind conditions), the system enters the approach phase where it heads to the target pointed directly into the estimated wind direction. Just before ground impact, the system transitions into the flare stage where both trailing edge brakes are actuated to maximum deflection in order to stall the canopy in order minimize the flight speed and hence the kinetic energy of the system at impact.

The lateral control algorithm implemented here uses the error between the desired path (given as a heading angle to track) and estimated heading to calculate the control command. This algorithm uses a nonlinear proportional and integral controller. The nonlinear proportional element tracks the desired heading and minimizes control input for small heading errors to prevent chattering while tracking a straight path. The integral controller is used to identify and overcome potential turn biases in the airdrop system which can be caused by uneven weight distribution or stretching of the rigging lines.

3.2. Conventional remote control

The conventional remote control (CRC) method uses a ground based human operator's visual recognition as a feedback signal to base control decisions. The operator is located near the IP in order to have a clear view of the target and surrounding airspace. An example of a human operator controlling the small-scale airdrop system during approach and landing is presented as a triptych in Fig. 3. This method capitalizes on human operators' innate ability to mentally apply a form of model predictive control by extrapolating the current position, orientation and velocity into a predicted path over a finite horizon. These visual cues which include ground wind sensing from a small wind streamer at the IP inform the operator how the system needs to be perturbed in order to steer the airdrop system to the target. This simple method replicates how conventional remote control operators fly drones in the hobby community and can be extended into airdrop operations by training ground crew that are present at the DZ to collect delivered supplies.

3.3. First person view

The first person view (FPV) video stream method simulates the ground based human operator controlling the airdrop system as if they were flying the system as a skydiver. Video feedback is provided by a GoPro camera with a fisheye lens which is mounted rigidly to the nose of the payload. This camera was chosen based on its light weight design and wide angle lens to provide the greatest field of view to the operator. A 5.8 GHz wireless transmitter



Fig. 3. Triptych showing the final landing sequence of a parafoil and payload system controlled by a ground based human operator using conventional remote control where $t_1 < t_2 < t_3$.



Fig. 4. Human operator using a computer display feedback method to inform control decisions.

sent onboard GoPro footage to a base station laptop. The IP was clearly designated with a 4.5 m “+” symbol made of polyester cloth and colored to provide high contrast against the ground marked the target.

Onboard video is provided to the operator using a high lumen, anti-glare display, exemplified in Fig. 4. The strong benefit of a digital display is that the operator is no longer required to be located at the DZ and could be located off site given proper communication connection and security protocols. This feedback method provides the operator with a bird’s eye view of the DZ while at high altitudes and detailed information on potential landing hazards as the vehicle drops altitude. In conjunction with the video stream, estimates from the aforementioned navigation algorithm are provided in a tabulated form. Included parameters were location with respect to the IP, altitude, horizontal components of the

wind, and descent rate. These estimates provided extra cues for the operator to help overcome potential challenges such as depth perception and high altitude terrain based navigation. As a note, transmitted video quality has sufficient pixel quality to identify the “+” IP marker from approximately 150 m and below but does not provide sufficient resolution to clearly identify the wind streamer direction seen in Fig. 3. Above this altitude, the operator must use terrain knowledge or tabulated data to steer the vehicle while at higher altitudes.

3.4. Live map

The goal of the live map (LM) method is to mimic common flight planning software used in the field of airdrop systems, most notably the FalconView software package [35]. This software is used for mission planning and can track aerial vehicles provided GPS data. The human operators are presented the digital interface in Fig. 5 which updates at 4 Hz on which to base control decisions. This method integrates navigation estimates into an aerial map to generate an accurate representation of the DZ and the vehicle movement. Current heading and course direction are displayed along with altitude, horizontal distance from the target, atmospheric wind magnitude and direction. Markers were added to the display at the start of flight testing each day to account for local obstacles that needed to be avoided while attempting to land at the IP. Additionally, breadcrumbs are placed at 1 Hz to show the recent trajectory of the vehicle.

3.5. Virtual cockpit display

The virtual cockpit display (VCD) method was designed as a user interface that blends both LM and FPV features in order to provide the most information to the human operator. With both a bird’s eye map of the DZ and a live FPV video stream from the

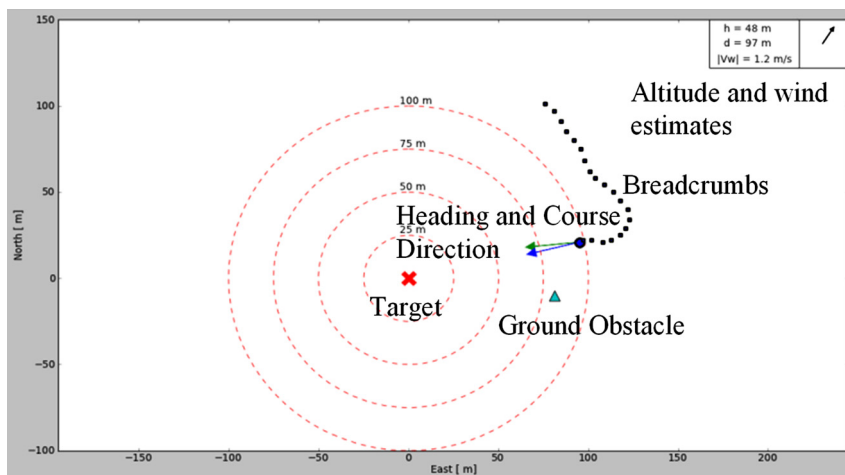


Fig. 5. Live map display showing system location, orientation, and relevant estimates.

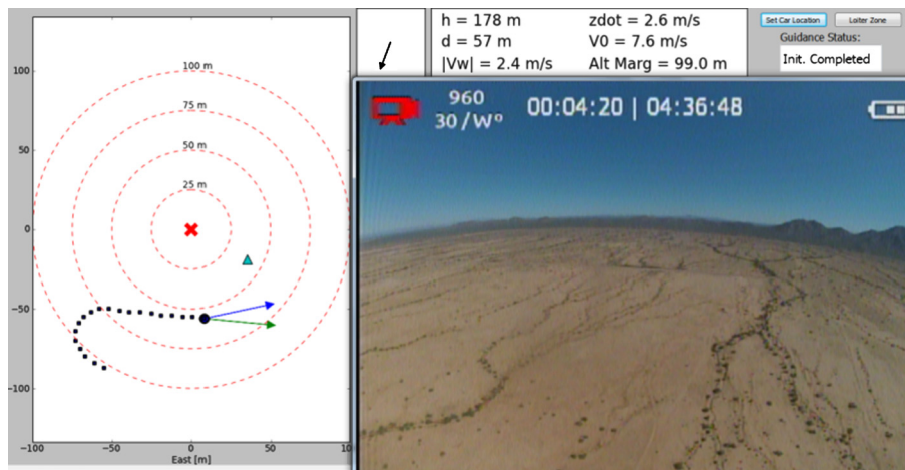


Fig. 6. Virtual cockpit display interface with both first person view and live map components.

payload, the human operator has the most information on the position and attitude of the airdrop system on which to base control decisions. A graphic of the display is shown in Fig. 6 with the LM on the left, FPV video stream on the right, and estimates from the navigation algorithm along the top. Included parameters were height above ground, horizontal distance to ground, wind magnitude and direction, descent rate, forward airspeed, and altitude margin. This final parameter is an estimate of the altitude that the vehicle would have over the target if it immediately flew from its current location to the IP. The remaining altitude, or altitude margin, provides the operator with the amount of altitude needed to be lost before flying to the target.

4. Experimental results

Flight test operations were conducted in flat desert terrain in Eloy, AZ and in a wooded clearing in the rolling hills outside of Atlanta, GA. Operations were conducted on cloudless days to provide operators clear views to and from the small scale airdrop system. All testing was conducted in an alternating fashion where a human operator would control the system for one drop, and the autonomous algorithm would control the next to ensure similar weather conditions across the data sets to accurately remove the impact of atmospheric conditions on operator performance in comparison to the autonomous algorithms. Landing capabilities of the operator are judge by both statistical accuracy metrics and through user feedback. From the results of several operators, indicators and display elements are identified which are key to an operator accomplishing the mission specifications. Landing accuracy is presented using landing dispersion plots with the axes rotated such that the vertical axis is aligned with the wind direction from each flight (denoted the Downwind direction). Statistics on landing accuracy are generated using the circular error probably (CEP) which is standard practice in the field of precision airdrop systems. The 50% (90%) CEP value is defined as the radius of a circle, centered at the IP, which contains 50% (90%) of the landing points. The 50% CEP is often referred to as the median miss and the 90% CEP characterizes an upper bound on system accuracy. A smaller CEP value indicates more landings closer to the target and a more accurate method.

Note that all methods required the navigation algorithm from the fully autonomous system to provide estimates to the operator and data logging purposes. This required the vehicle to run the open loop initialization procedure before manual control was passed to the operator.

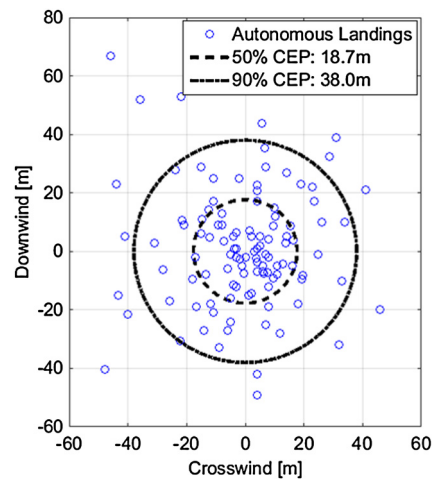


Fig. 7. Aggregate landing dispersion of a fully autonomous airdrop system.

4.1. Fully autonomous

The results of an autonomous system are presented to create a baseline to analyze the potential benefits from human-in-the-loop control of guided airdrop systems. A total of 142 autonomous flights were conducted across testing of all human-in-the-loop methodologies. Atmospheric winds varied substantially and ranged from benign to gusty conditions in which turbulent winds reached over 6 m/s (approximately 80% of the vehicle airspeed). The landing dispersion is presented in Fig. 7 along with circles indicating 50% and 90% CEP.

Landing points show a relatively uniform distribution around the IP and resulted in a 50% CEP of 18.7 m and a 90% CEP of 38.0 m. While these indicate impressive landing accuracy values, this system was blind to objects around the IP, primarily the ground station where a vehicle was parked and human operators were located. Several autonomous airdrops required human intervention at landing to ensure the experimental system didn't collide with the ground station. All other drops landed in wings level flight and almost all flights had a proper flare to ensure smooth landing. Several flights exhibited incorrect flare altitude due to drift in the barometric altimeter causing the system to land at the IP harder than normally observed.

In order to perform an equivalent comparison between the conventional autonomous system and human operators, statistics from individual flight test campaigns are used. While it is the goal to test system performance in a variety of atmospheric wind condi-

Table 1
Landing statistics of all autonomous and human-in-the-loop methods.

Feedback method	Human operator		Autonomous system		Accuracy improvement achieved by human operator in 50% CEP
	50% CEP (m)	90% CEP (m)	50% CEP (m)	90% CEP (m)	
CRC	10.4	21.0	17.7	38.0	41%
FPV	16.4	46.0	16.5	31.6	0%
LM	19.2	43.2	25.7	57.4	25%
VCD	16.9	37.7	21.6	45.3	22%

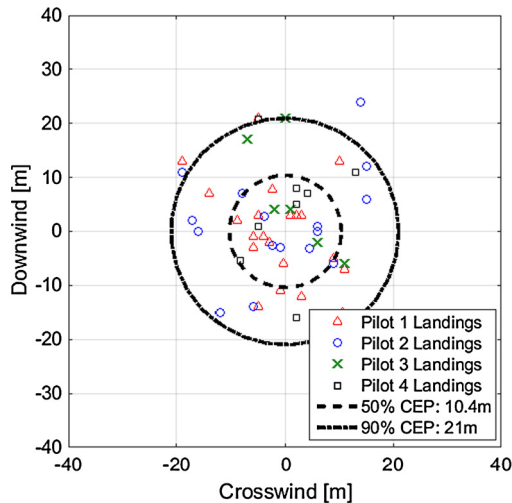


Fig. 8. Landing dispersion of four human operators controlling a small scale airdrop system using the conventional remote control method.

tions, certain flight test operations experienced calmer or gustier conditions than others. Typically, the landing accuracy for autonomous systems decrease in more intense and variable wind fields as it poses a greater disturbance to the control system. The same is expected for the human-in-the-loop control of guided airdrop systems. Hence, the concurrently tested conventional autonomous system landing statistics are used as a baseline for each operator feedback method since flight test operations are conducted in an alternating format as described in Section 3. A list of all individual landing accuracy statistics from flight test operations is presented in Table 1.

4.2. Conventional remote control

The ability of an operator to accurately guide a parafoil and payload system to the target is studied in this section. Four operators were used, with skill levels intermediate to advanced, to directly steer the vehicle to the IP. 52 flights were conducted between the four pilots and the landing dispersion is presented in Fig. 8 where each operator is denoted by a different marker and aggregate CEP circles are presented.

Individual human operator 50% CEP values ranged from 9.1 m to 10.8 m; the aggregate 50% CEP was 10.4 m and the 90% CEP was 21.0 m. This method exhibited a drastic 41% improvement in accuracy in comparison to the autonomous system. The landing dispersion was centered on the target indicating that the human operators were able to consistently land the system in the region of the target. The CRC method is both an accurate and simple method as it relies directly on the operators direct sensing of the airdrop system in the airspace above the DZ.

Additional information on the CRC method is based upon qualitative feedback received by the operators. A concise summary of responses indicated the following.

1. The transition from loitering near the target to final approach was difficult to properly gauge.
2. Offset position of the operator from the IP caused depth perception issues.
3. Desired landing direction was easy to determine as the operator was physically buffeted by the same winds hitting the airdrop system at low altitudes.

These observations bring to light that the primary driver of operator uncertainty in the CRC method is based on perception of the aerial vehicle, not wind estimation which is the primary driver of error in autonomous systems. The human operator is robust (in the sense of conventional controller design) to state estimation error since operators had low confidence in the accuracy of their location estimates but were still able to guide the system to the target. Only ground wind information was easily identifiable as the operator was physically standing at the DZ. This information allowed operators to easily align the vehicle with the ground wind direction to slow the vehicle ground speed prior to landing. Vision of the system and environment allowed operators to consistently land in level flight with a properly timed flare maneuver. Operators also indicated that obstacle avoidance near the target was not difficult to achieve. Human control performs obstacle avoidance in a very simple manner while it is very computationally expensive to implement in guidance logic.

This method could be further improved if an operator visually spotting the system was also provided with onboard estimates to further enhance their knowledge of the system in space. Onboard state estimates could easily be conveyed to the operator via a small display or audibly via a ground station interfacing with the payload. The following methods expand upon this idea of onboard feedback to create human-in-the-loop control schemes that do not require the operator to physically be at the DZ.

4.3. First person view

Experiments using the front mounted camera for video feedback to the ground station were conducted by three operators with general skill levels between intermediate and advanced. None of the operators had used this method significantly prior to experimental testing. Landing dispersion plots of 43 total flights are presented in Fig. 9. Combining the results of all three operators, the FPV method exhibited a 50% CEP of 16.4 m and a 90% CEP of 46.0 m. Operators performed nearly equivalently to the concurrently tested autonomous algorithm which had a 50% CEP of 16.5 m and 90% CEP of 31.6 m.

Using this method, operators tended to miss the target short indicating that they were not as capable at constructing a set of commands to accurately reach the target. Operators using FPV feedback successfully avoided hazards near the IP including the test vehicle and base station, large shrubs, and cacti. Qualities of this display that helped human operators maintain autonomous level accuracy is summarized below based on operator feedback.

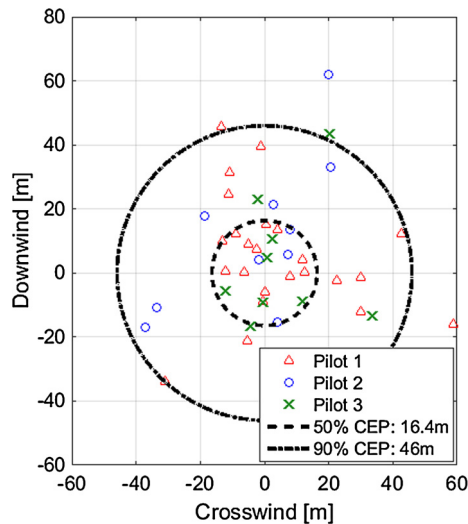


Fig. 9. Landing dispersion of three human operators using first person view video feedback.

1. The FPV video stream provided a clear understanding of the DZ when at altitude including the ability to identify and track major obstacles that should be avoided.
2. Users were not confident in their ability to estimate wind velocity from the video alone unless the magnitude was near the parafoil airspeed. Altitude was also difficult to estimate due to lack of depth perception.
3. Loss of the IP from the camera field of view had potential to cause disorientation after exiting a turn if no other clear marker (e.g. a hazard) was easily recognizable.
4. It was difficult for the human operators to mentally reconcile the FPV video stream with tabulated onboard estimates. In particular, the camera view is relative to the orientation of the payload while the onboard estimates were in inertial space.

The use of video feedback as the main element of feedback provided the operator with a great understanding of the airspace but did not sufficiently present data in a way to improve accuracy over the autonomous algorithm. Operators primarily used the FPV feedback display to make decisions and tabulated estimates as a secondary reference as both were difficult to track simultaneously. Tabulated estimates were primarily used to identify the atmospheric winds which were not easily identifiable based on the video stream alone. Lack of clear wind feedback is the primary driver why operator landings have a slight clumping downwind of the target as seen in Fig. 9. Additionally, operators had a common tendency to oversteer because they would hold a control input until a certain reference was back in the field of view. After releasing the command, the natural turn rate dynamics carried the vehicle past the desired heading and the operator had to reverse command. When this occurred at low altitudes where the area of land in the field of view was more limited, issues highlighted in point 3 causes an increase in 90% CEP miss distance. Last, while depth perception was difficult at high altitudes, it was very clear at short distances allowing operators a clear indication of when to flare the vehicle for smooth landing.

4.4. Live map

Having identified the strengths and weaknesses of the previously analyzed methods, the goal of the LM method is to provide the human operator with increased spatial awareness of the airdrop system and surrounding area, particularly in the horizontal plane. A graphical user interface (GUI) was created to display real-

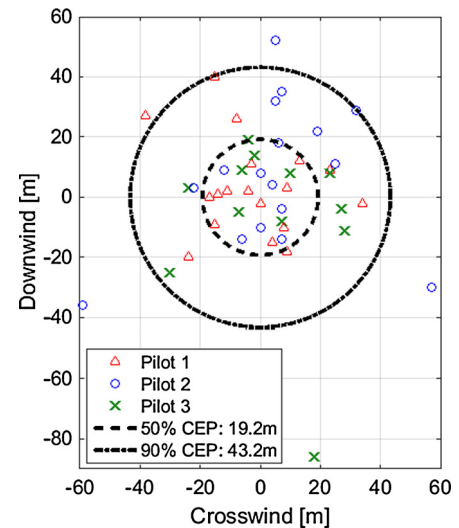


Fig. 10. Landing dispersion of three human operators using the live map feedback method.

time updates of the current location and heading of the aerial vehicle in the drop zone. Three pilots, with skill levels again ranging from intermediate to advanced (based on prior experience and not specifically related to this method), controlled the airdrop system to the IP with the proposed method. Landing dispersion plots are presented in Fig. 10 with circles denoting 50% and 90% CEP. Human operators were able to land 25% more accurately than the fully autonomous system with a 50% CEP of 19.2 m and 90% CEP of 43.2 m. The landing points are relatively dispersed in the region around the IP with no particular clumping. The four major outliers are a result of the human operators learning to use the LM feedback method as the landings occurred early in the flight testing.

As with the previous studies, operator feedback was gathered to gain insight on the elements of the display that were beneficial to meet the mission objectives. A summary of the main points listed by operators is presented below.

1. Atmospheric wind direction and relative magnitude (with respect to vehicle airspeed) was clearly identifiable based on the distortion of the breadcrumb trail.
2. Markers for ground hazards were easy to identify and avoid during final approach.
3. A slight disconnect between the physical system and operator was apparent and manifested in lateral control errors while steering the vehicle.

With the use of breadcrumbs, human operators are able to clearly see the impact of wind on the trajectory of the vehicle. Breadcrumbs have greater separation when the vehicle is flying with the wind (due to greater inertial velocity) and are closer together when flying into the wind. With wind knowledge (from both breadcrumbs and displayed navigation estimates) and a clear representation of the vehicle location with respect to the target, operators were confident in their ability to steer the vehicle to the IP. Point 2 highlights the ability of markers to provide obstacle references to avoid during landing. This could be expanded by importing terrain maps and having the obstacle pattern change with altitude.

Last, point 3 indicated a disconnect between the physical system and the human operator. Operators exhibited issues with oversteering the vehicle, similar but more pronounced than what was observed in the case of FPV feedback. The LM display primarily shows the steady state turn rate behavior of the vehicle though the heading vector and arcing of breadcrumbs behind the system. After an asymmetric input has been commanded by an operator, it

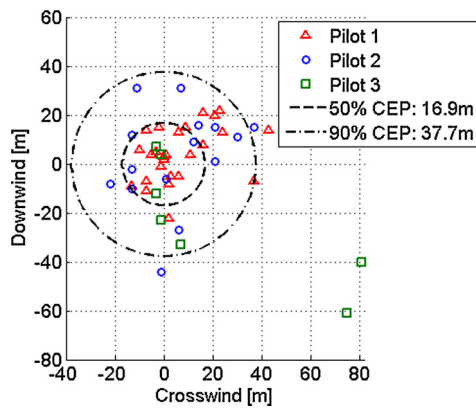


Fig. 11. Landing dispersion of three human operators using the virtual cockpit display method.

can take approximately 1 second for the map to display the resulting turn due to the lateral dynamics of the parafoil. As a result of this time delay, the operator would often command sequentially large values as a result of the system appearing unresponsive only to then have the vehicle enter a sharp turn and pass the desired heading. This problem was not observed in the FPV feedback method as a slight roll of the camera was quickly noticeable by operators after commanding an asymmetric brake input. The second manifestation of the disconnect between operator and system appeared during final approach. In early flights, operators were prone to make aggressive maneuvers to minimize the miss distance resulting in harsh impacts. Operators were able to overcome both issues through training, but proved to be a disadvantage of this method.

4.5. Virtual cockpit display

The goal of the VCD method is to combine the FPV and LM feedback methods into a unified display where the combined benefit overcomes the individual difficulties using just one method. In particular, the FPV method provided a strong body centric feedback that provided the operator with a strong connection to the vehicle while the LM method gave the operator a clear global sense of the vehicle's position and atmospheric winds with respect to the target. For this study, one novice operator and two advanced operators used the VCD display to control the airdrop system to the target. The novice operator had minimal flight experience but knowledge of human interfaces whereas the two advanced operators had significant flight experience and had tested the previous two methods as well giving them significant preparation for this task. The landing dispersion of the three operators are presented in Fig. 11 with a general tight clumping around the IP except for two significant outliers that occurred during several of the novice operators initial flights.

With the VCD method, the combined 50% CEP for all users was 16.9 m, a 22% improvement over the conventional autonomous system tested during the same flight test session. The 90% CEP was reduced to 37.7 m which is a strong improvement considering two large misses by the novice operator during initial flight testing. If the two outliers are rejected as part of the learning processes, the results show a 50% CEP of 16.1 m and 90% CEP of 32.9 m. Overall, these results improve upon the FPV method and exhibited a nearly equivalent improvement as the LM method.

Qualitative information from operators was used to understand their interactions with the VCD method and further understand the landing statistics. A summary of human operator responses are presented below.

1. Having multiple display components was important as each was most beneficial during different segments of the flight. LM component was most useful at altitude. At intermediate altitudes, the FPV allowed the user to survey the DZ while the LM helped maintain spatial awareness and prevented disorientation. During approach the FPV stream along with the tabulated indicators of altitude and glide slope were the most valuable.
2. Users felt confident in understanding where the airdrop system was and was heading in the airspace above the DZ. However, slight user discomfort was noted when mentally reconciling the inertial representation of the LM and the body centric view of the FPV.
3. The largest difficulty was handling changes to the wind magnitude and direction below the current altitude.

The combination of both methods successfully provided the human operator with a clear understanding of the airspace above the DZ including the parafoil system itself and any potential obstacles to avoid. In particular, the primary issue of each method was solved by using feedback from the other method. Disorientation at low altitude seen in FPV testing was completely removed due to the LM and over steering was greatly reduced with video feedback of showing what was ahead of the airdrop system. With the addition of the FPV, the operator is able to base control decisions on numerous hours driving ground vehicles due to the perspective it offers. The FPV video stream also helped understand the transient dynamics as the roll was noticeable before the steady state turn rate was visible in the LM. Most importantly, this method was the first in which the operator was able to comfortably understand the position and dynamics of the guided airdrop system enabling operators to focus on future conditions of the wind velocity closer to ground level. This is important as it represents the primary driver of landing error in autonomous systems. Facing the same challenges as the conventional autonomous system, the 22% improvement by the human user is significant. The user also expressed slight difficulty mentally reconciling the LM with the FPV. In situations where the vehicle was flying south, the LM indicator showed the vehicle moving down the page while the FPV stream always gives a sense of moving forward, or up the screen. Occasionally this caused an operator to turn in the incorrect direction briefly before correcting. Future work into improved fusion of data streams, such as plotting the LM on different coordinate axes is expected to further improve this method.

A summary of all the landing statistics of each method is presented in Table 1 with a comparison against the conventional autonomous system tested concurrently.

5. Conclusion

It has been shown that semi-autonomous, human control is capable of achieving superior landing accuracy compared to a state of the art, fully autonomous airdrop system. This was established through a series of flight test experiments that were trialed by multiple human operators. The four human-in-the-loop control modalities explored in this work were conventional remote control (operator at the drop zone looks up to visually track the aerial vehicle), first person view (a real-time camera feed from the payload is supplied to the operator), live map (GPS based bird's eye map of the drop zone), and virtual cockpit display (a combination of first person view and live map). These feedback methods influenced operator control decisions to satisfy the goal of minimizing system landing error and maximizing payload survivability. The conventional remote control method proved to be the most effective method with a 41% improvement over the autonomous system but requires the operator to be both physically present at the drop

zone and able to see the aerial vehicle from the ground. The digital display methods found that operators were most certain of their actions and accurate when provided both the live map and first person view feedback as in the virtual cockpit display. Additionally, key metrics used by operators were established to be the altitude margin (which aids operators in deciding when to fly towards the target), altitude, and atmospheric wind direction and magnitude. It is expected that further fusion of the available data into a seamless interface would continue to improve operators' landing capabilities making human-in-the-loop control a strong candidate for achieving precision payload delivery.

Conflict of interest statement

There are no conflicts of interest with this work.

Acknowledgements

The authors would like to acknowledge the support of the Natick Soldier Research, Development and Engineering Center (NSRDEC) Airdrop Technology Team.

References

- [1] C. Boggs, Computed air release point data collection, post processing and applications, in: AIAA Aerodynamic Decelerator Systems Technology Conference, AIAA, Daytona Beach, FL, 2015.
- [2] P. Hattis, et al., Status of an On-Board PC-Based Airdrop Planner Demonstration, AIAA paper 2066, 2001, pp. 22–24.
- [3] O.A. Yakimenko, et al., Synthesis of optimal control and flight testing of an autonomous circular parachute, *J. Guid. Control Dyn.* 27 (1) (2004) 29–40.
- [4] G. Brown, et al., The affordable guided airdrop system (AGAS), in: 15th CEAS/AIAA Aerodynamic Decelerator Systems Technology Conference, 1999.
- [5] W. Barton, C. Knapp, Controlled recovery of payloads at large glide distances, using the para-foil, *J. Aircr.* 5 (2) (1968) 112–118.
- [6] T.F. Goodrick, A. Murphy, Analysis of various automatic homing techniques for gliding airdrop systems with comparative performance in adverse winds, in: American Institute of Aeronautics and Astronautics, Aerodynamic Deceleration Systems Conference, 4th, Palm Springs, Calif., 1973.
- [7] T. Goodrick, Estimation of wind effect on gliding parachute cargo systems using computer simulation, in: AIAA Aerodynamic Decelerator Systems Conference, 1970.
- [8] T. Goodrick, Hardware options for gliding airdrop guidance systems, in: 6th AIAA Aerodynamic Decelerator and Balloon Technology Conference, 1979.
- [9] J.R. Hogue, H.R. Jex, Applying parachute canopy control and guidance methodology to advanced precision airborne delivery systems, in: AIAA Aerodynamic Decelerator Systems Technology Conference, 1995.
- [10] J.E. Murray, et al., Further Development and Flight Test of an Autonomous Precision Landing System Using a Parafoil, vol. 4599, National Aeronautics and Space Administration, Office of Management, Scientific and Technical Information Program, 1994.
- [11] A. Calise, D. Preston, Design of a Stability Augmentation System for Airdrop of Autonomous Guided Parafoils, AIAA Paper 6776, 2006.
- [12] A.J. Calise, D. Preston, Swarming/flocking and collision avoidance for mass airdrop of autonomous guided parafoils, *J. Guid. Control Dyn.* 31 (4) (2008) 1123–1132.
- [13] N. Slegers, M. Costello, Aspects of control for a parafoil and payload system, *J. Guid. Control Dyn.* 26 (6) (2003) 898–905.
- [14] M. Ward, Adaptive Glide Slope Control for Parafoil and Payload Aircraft, Georgia Institute of Technology, 2012, p. 138.
- [15] M. Ward, et al., Flight test results of recent advances in precision airdrop guidance, navigation, and control logic, in: Aerodynamic Decelerator Systems, Daytona Beach, FL, 2015.
- [16] J. Rogers, N. Slegers, Terminal guidance for complex drop zones using massively parallel processing, in: Aerodynamic Decelerator Systems Technology Conferences, American Institute of Aeronautics and Astronautics, 2013.
- [17] T.A. Herrmann, et al., Utilizing ground-based LIDAR for autonomous airdrop, in: AIAA Aerodynamic Decelerator Systems (ADS) Conference, American Institute of Aeronautics and Astronautics, 2013.
- [18] R. Chipalkatty, et al., Human-in-the-loop: MPC for shared control of a quadruped rescue robot, in: 2011 IEEE/RSJ International Conference on Intelligent Robots and Systems (IROS), IEEE, 2011.
- [19] K. Hirai, et al., The development of Honda humanoid robot, in: 1998 IEEE International Conference on Robotics and Automation, 1998, Proceedings, IEEE, 1998.
- [20] P. Griffiths, R.B. Gillespie, Shared control between human and machine: haptic display of automation during manual control of vehicle heading, in: 12th International Symposium on Haptic Interfaces for Virtual Environment and Teleoperator Systems, 2004, HAPTICS'04, Proceedings, IEEE, 2004.
- [21] N. Diolaiti, C. Melchiorri, Teleoperation of a mobile robot through haptic feedback, in: Haptic Virtual Environments and Their Applications, IEEE International Workshop 2002 HAVE, IEEE, 2002.
- [22] S.-G. Hong, et al., Artificial force reflection control for teleoperated mobile robots, *Mechatronics* 8 (6) (1998) 707–717.
- [23] R. Mayer, Terminal descent controlled vehicle recovery, in: 8th Aerodynamic Decelerator and Balloon Technology Conference, 1984.
- [24] R.T. Mayer, E. Puskas, P. Lissaman, Controlled terminal descent and recovery of large aerospace components, in: 9th Aerodynamic Decelerator and Balloon Technology Conference, 1986.
- [25] M. Cahillane, C. Baber, C. Morin, Human factors in UAV, in: Sense and Avoid in UAS: Research and Applications, vol. 61, 2012, p. 119.
- [26] M. Draper, et al., Manual versus speech input for unmanned aerial vehicle control station operations, in: Proceedings of the Human Factors and Ergonomics Society Annual Meeting, SAGE Publications, 2003.
- [27] K. Funabiki, T. Iijima, T. Nojima, Method of trajectory generation for perspective flight-path display in estimated wind condition, *J. Aerosp. Inform. Syst.* 10 (5) (2013) 240–249.
- [28] B.L. Harrison, et al., Transparent layered user interfaces: an evaluation of a display design to enhance focused and divided attention, in: Proceedings of the SIGCHI Conference on Human Factors in Computing Systems, ACM Press/Addison-Wesley Publishing Co., 1995.
- [29] J.S. McCarley, C.D. Wickens, Human Factors Concerns in UAV Flight, Institute of Aviation, University of Illinois, Urbana-Champaign, IL, 2004.
- [30] M. Cummings, et al., Automation Architecture for Single Operator, Multiple UAV Command and Control, DTIC Document, 2007.
- [31] A. Franchi, et al., Shared control: balancing autonomy and human assistance with a group of quadrotor UAVs, *IEEE Robot. Autom. Mag.* 19 (3) (2012) 57–68.
- [32] OSD, O.O.T.S.O.D., Unmanned Aircraft Systems Roadmap, 2005–2030, DOD, Washington, 2005.
- [33] M.R. Cacan, et al., Autonomous airdrop systems employing ground wind measurements for improved landing accuracy, *IEEE/ASME Trans. Mechatron.* (2015).
- [34] M. Ward, M. Costello, N. Slegers, On the benefits of in-flight system identification for autonomous airdrop systems, *J. Guid. Control Dyn.* 33 (5) (2010) 1313–1326.
- [35] FalconView, Available from <https://www.falconview.org/trac/FalconView>, November 13, 2014.